

# Microtrap on a concave grating reflector for atom trapping\*

Hui Zhang(张慧)<sup>1</sup>, Tao Li(李涛)<sup>2</sup>, Ya-Ling Yin(尹亚玲)<sup>1</sup>,  
Xing-Jia Li(李兴佳)<sup>1</sup>, Yong Xia(夏勇)<sup>1,†</sup>, and Jian-Ping Yin(印建平)<sup>1</sup>

<sup>1</sup>State Key Laboratory of Precision Spectroscopy, Department of Physics, East China Normal University, Shanghai 200062, China

<sup>2</sup>National Laboratory of Solid State Microstructures, College of Engineering and Applied Sciences, Nanjing University, Nanjing 210093, China

(Received 21 February 2016; revised manuscript received 12 April 2016; published online 25 June 2016)

We propose a novel scheme of optical confinement for atoms by using a concave grating reflector. The two-dimension grating structure with a concave surface shape exhibits strong focusing ability under radially polarized illumination. Especially, the light intensity at the focal point is about 100 times higher than that of the incident light. Such a focusing optical field reflected from the curved grating structure can provide a deep potential to trap cold atoms. We discuss the feasibility of the structure serving as an optical dipole trap. Our results are as follows. (i) Van der Waals attraction potential to the surface of the structure has a low effect on trapped atoms. (ii) The maximum trapping potential is  $\sim 1.14$  mK in the optical trap, which is high enough to trap cold  $^{87}\text{Rb}$  atoms from a standard magneto-optical trap with a temperature of 120  $\mu\text{K}$ , and the maximum photon scattering rate is lower than 1/s. (iii) Such a microtrap array can also manipulate and control cold molecules, or microscopic particles.

**Keywords:** subwavelength structures, high-contrast gratings, beam focusing, laser trapping

**PACS:** 78.67.Pt, 92.60.Ta, 87.80.Cc, 37.10.Gh

**DOI:** 10.1088/1674-1056/25/8/087802

## 1. Introduction

In recent years, the grating has become a hot optical element in a wide range of applications such as filters,<sup>[1]</sup> vertical-cavity surface-emitting lasers,<sup>[2,3]</sup> high-efficiency photodetector,<sup>[4,5]</sup> and the grating magneto-optical trap.<sup>[6]</sup> Especially a kind of high-contrast grating (HCG) comprised of high-index grating completely surrounded by low-index materials, possesses extraordinary features: the ultra-broadband ( $\Delta\lambda/\lambda > 30\%$ ), high reflectivity ( $> 99\%$ ), and the ultra-high quality factor resonances.<sup>[7]</sup> Such striking optical features are attractive for various applications. A non-periodic flat grating reflector with focusing ability is first demonstrated.<sup>[8]</sup> An important property of flat HCG is that the wavefront phase of the reflected (or transmitted) light can be manipulated while maintaining a high reflectivity (or transmittance). With the precise adjustment of the structural parameters of HCG such as the grating period and filling factor, it is possible to create a parabolic wavefront phase and achieve an excellent focusing ability. Subsequently, the focusing performances for different kinds of flat grating reflectors have been extensively studied.<sup>[9–14]</sup> As is well known that when a two-level atom moves in an inhomogeneous light field, it will experience an optical dipole force and be attracted towards the maximum of the optical field.<sup>[15]</sup> Such a strong focusing optical field reflected from the flat (or curved) grating structure can provide the deep potential to trap the cold atoms, molecules and particles, so it would be interesting and worthwhile to de-

sign some controllable optical traps based on the grating meta-surfaces and explore their potential applications in the fields of atom, molecule, and quantum optics. In this paper, a novel scheme of optical trapping for atoms by using a concave grating reflector is proposed and studied numerically. The grating reflector with the curved dielectric ring patterns not only obtains excellent focusing ability, but also can maintain high reflectivity. The favorable advantage of our scheme is that the light intensity reflected from the curved grating structure at the focal point is much higher than that from the flat one. Our study shows that such a focusing optical field can provide the deep potential to trap cold atoms.

## 2. Scheme of a strong optical confinement for atoms using a concave grating reflector

We first present a resonant sub-wavelength grating structure that acts as a broadband reflector, which comprises a high-index material fully surrounded by a low index material, such as Si/air, depicted in Fig. 1(a). The Si grating is determined by its parameters including period  $T$ , Si-bar width  $t$ , filling factor  $f = t/T$ , and grating thickness  $d$ . The optical property in this structure depends on the ratio of period  $T$  to wavelength  $\lambda$ . In the short wavelength range ( $\lambda \ll T$ ), this grating acts as a diffraction grating. In the long wavelength limit ( $\lambda \gg T$ ), the structure behaves like a homogeneous layer with an effective refractive index. However, in the subwavelength regime, the grating behaves sharply differently, and exhibits broadband

\*Project supported by the National Natural Science Foundation of China (Grant Nos. 11374100, 91536218, and 11274114) and the Natural Science Foundation of Shanghai Municipality, China (Grant No. 13ZR1412800).

†Corresponding author. E-mail: [yxia@phy.ecnu.edu.cn](mailto:yxia@phy.ecnu.edu.cn)

and high reflectivity which is not attributed to gratings.<sup>[16,17]</sup> As shown in Fig. 1(b), we calculate the effects of grating width  $t$  and incident wavelength  $\lambda$  on reflectivity when  $T = 1 \mu\text{m}$  and  $d = 200 \text{ nm}$  by using the finite difference time domain (FDTD) method. In the figure, several obvious boundaries are observed, which illustrates that the optical properties of the grating can make sharp transformation with the change of  $t$ . The reflectivity distribution also depends on the thickness  $d$  of the grating. For achieving high reflectivity, the HCG thickness should be properly chosen such that a destructive interference

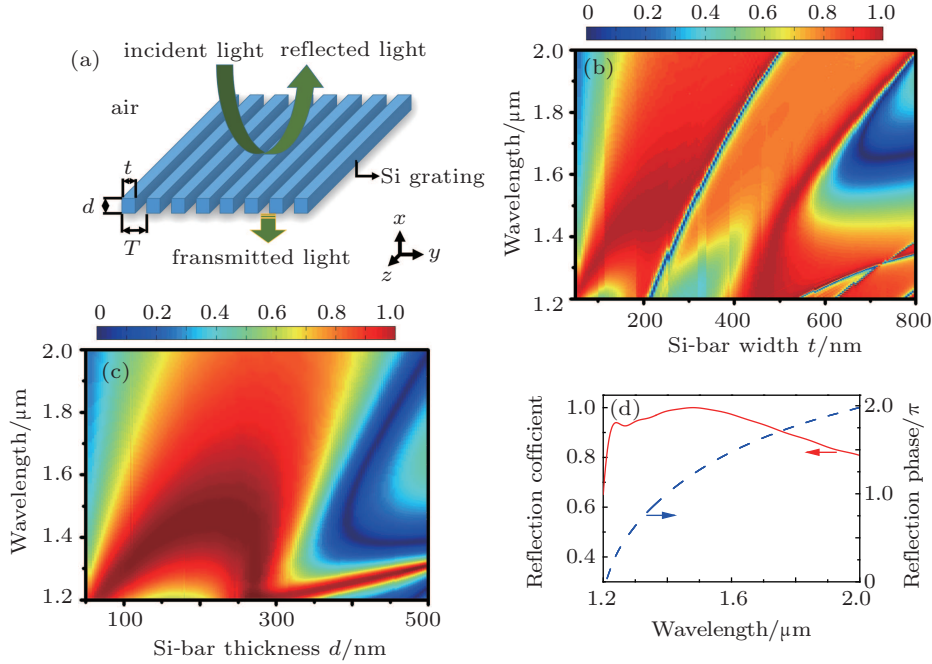


**Fig. 1.** (color online) (a) Schematic diagram of a planar HCG structure on a subwavelength scale under incident beam with  $E$ -field polarization perpendicular to the grating bars. (b) The reflectivity distributions calculated by FDTD method for the Si-bar width  $t$  in a range from 50 nm to 800 nm and wavelength from 1.2  $\mu\text{m}$  to 2.0  $\mu\text{m}$ . (c) The reflectivity distributions for the Si-bar thickness  $d$  in a range from 50 nm to 500 nm and wavelength from 1.2  $\mu\text{m}$  to 2.0  $\mu\text{m}$ . (d) Reflection coefficient and phase for a strictly periodic Si grating with  $T = 1 \mu\text{m}$ ,  $t = 200 \text{ nm}$ , and  $d = 250 \text{ nm}$ .

A reflector of one-dimension flat grating structure has high reflectivity and a wide wavelength-tuning bandwidth, and it can be extended to two-dimensional (2D) grating structure with a concave surface shape. By locally tuning the filling factor, the reflection phase of the mirror is tailored to a parabolic distribution to the position while the reflectivity magnitude remains high everywhere, so that the reflector not only maintains a high reflectivity, but also obtains excellent focusing ability. We design a ring grating structure, namely, 2D concave dielectric-ring reflector, depicted in Fig. 2(a). Here, the geometrical shape of HCG structure is expressed as

$$x + \sqrt{x^2 + y^2} = 2L. \quad (1)$$

In Eq. (1),  $L$  denotes the focal length, and the focal point is the origin of coordinates. Then we can give the spatial phase-difference formula from the incident wavefront to the focal point below,

$$\Delta\phi(x) = \phi(x) - \phi(0) = \frac{2\pi n_F}{\lambda} (H + L), \quad (2)$$

is obtained at the exit plane, which cancels transmission.<sup>[18]</sup> Figure 1(c) shows the effects of grating thickness  $d$  and incident wavelength  $\lambda$  on reflectivity when we fix  $T = 1 \mu\text{m}$  and  $t = 250 \text{ nm}$ , and an S-shaped high-reflection region can be obviously observed and the reflectivity is very high in a wide wavelength range, which can be tuned by adjusting the reasonable parameters. Figure 1(d) shows that the reflectivity is greater than 90% in a wide incident wavelength range from 1.3  $\mu\text{m}$  to 1.6  $\mu\text{m}$  and the corresponding reflection phase.

where  $\lambda$  is the wavelength of the incident light,  $L$  is the focal length,  $n_F$  is the refractive index of the medium, and  $H$  is the distance from the incident wavefront to the bottom of the curved grating. The desired  $\Delta\phi(x)$  based on Eq. (2) is indicated in Fig. 2(b). The design of the concave grating reflector requires a constant phase of  $1.38\pi$  from center to edge for focal length  $L = 10.5 \mu\text{m}$  at the incident wavelength  $1.55 \mu\text{m}$ .

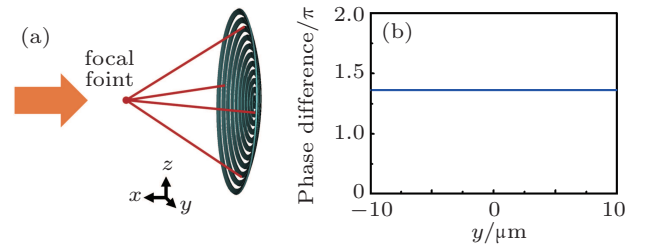


**Fig. 2.** (color online) (a) Schematic diagram of an HCG focusing dielectric-ring reflector. (b) Reflection phase-difference for focal length  $L = 10.5 \mu\text{m}$ .

The spatial distribution of the optical field reflected by the ring-grating can be determined from Maxwell's wave equation

and simulated by using FEM software packages. In order to facilitate integrating an optical atom chip, at the bottom of the 11-ring grating structure with an upper diameter of 11  $\mu\text{m}$  and a depth of 2.88  $\mu\text{m}$ , we add a  $\text{SiO}_2$  substrate, shown in Fig. 3. Here, the focal length of the structure is fixed to be 10.5  $\mu\text{m}$ .

Figures 4(a) and 4(b) show the optical intensity distributions at the  $xy$  plane ( $z = 0$ ) and the focal plane ( $yz$  plane, and  $x = 0$ ), respectively, which exhibits excellent focusing ability. Figures 4(c) and 4(d) show one-dimensional (1D) relative optical intensity distributions along the  $x$  and  $y$  axis at the focusing point for Figs. 4(a) and 4(b), respectively. At the focal plane, the full width at half maximum (FWHM) of the optical intensity distribution is 0.849  $\mu\text{m}$ . The light intensity at the focal point is about 100 times higher than that of the incident light. Thus, such strong focusing optical field reflected from the curved grating structure can provide the deep potential to

trap the cold atoms, molecules and particles.

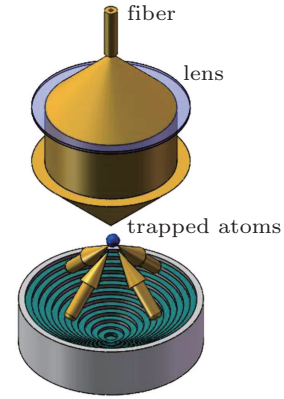


**Fig. 3.** (color online) Schematic diagram of a three-dimensional (3D) optical focusing trapping with adding a  $\text{SiO}_2$  substrate under radially polarized illumination.

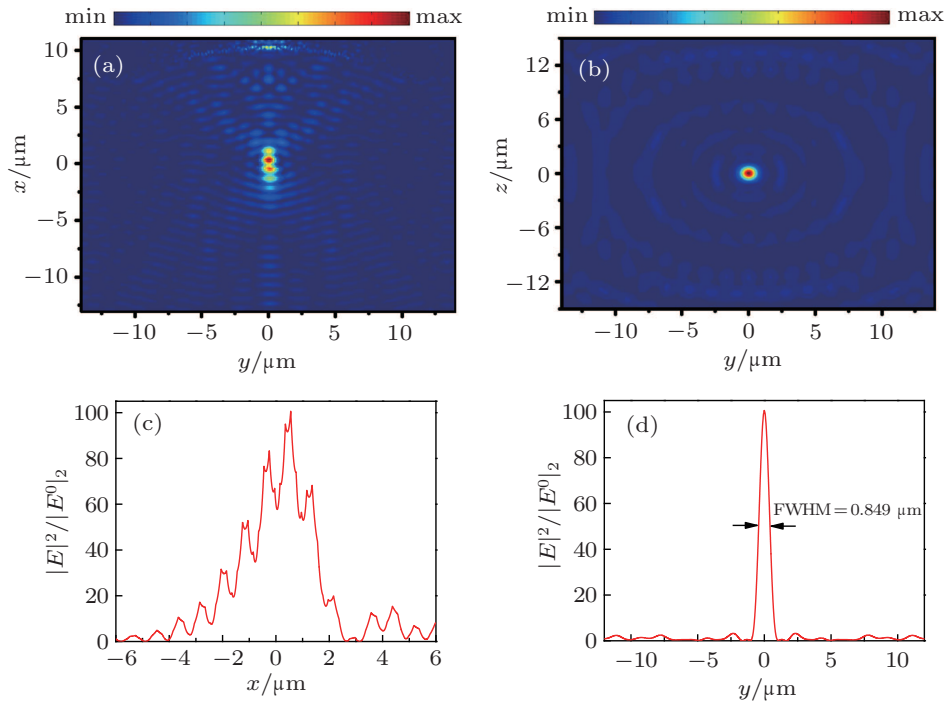


**Fig. 4.** (color online) (a) and (b) 2D intensity distributions of the focused beam on the  $xy$  and  $yz$  planes respectively, when plane wave illuminates from the curved Si-grating side. The wavelength of the incident light is 1.55  $\mu\text{m}$ . (c) and (d) 1D relative intensity distributions on the  $x$  and  $y$  axis at the focusing point for panels (a) and (b) respectively.

### 3. Feasibility and discussion

We discuss the feasibility of the concave grating structure serving as an optical dipole trap.

#### 3.1. Optical potential, dipole force and scattering rate

When a neutral atom is placed into an optical field, it interacts with an electric field  $\mathbf{E}$ , experiencing a dipole potential given by<sup>[15]</sup>

$$U_{\text{dip}} = -\frac{1}{2} \langle \mathbf{p} \mathbf{E} \rangle = -\frac{1}{2\epsilon_0 c} \text{Re}(\alpha) I, \quad (3)$$

$$\mathbf{F}_{\text{dip}}(\mathbf{r}) = -\nabla U_{\text{dip}}(\mathbf{r}) = \frac{1}{2\epsilon_0 c} \text{Re}(\alpha) \nabla I(\mathbf{r}). \quad (4)$$

Here  $\alpha$  is the atom polarizability,  $\mathbf{p}$  is the dipole moment, and  $I$  is the field intensity. The dipole force results from the gradient of the potential, which is a conservative force and proportional to the intensity gradient of the field. When the light field is red detuned, the interaction potential is attractive, and the atoms will be attracted towards the maximum of the light field. Therefore, atoms will be trapped at a red-detuned focusing point. Taking  $^{87}\text{Rb}$  for instance, setting the laser light:  $P = 100$  mW and  $w_0 = 20$   $\mu\text{m}$ , according to Eqs. (3) and (4), we can calculate the dipole potential and the dipole force, and the results are shown in Fig. 5. We obtain the maximum trapping potential to be  $\sim 1.14$  mK, which is high enough to

trap cold  $^{87}\text{Rb}$  atoms from a standard magneto-optical trap with a temperature of 120  $\mu\text{K}$ , and a maximum dipole force  $F(y)_{\text{max}} = 2.8 \times 10^{-23}$  N, which is at least 20 times the gravity force exerted on Rb atoms. This shows that  $F(y)$  is strong enough to balance the action of the gravity force on the atoms.

However, as the laser frequency is detuned further and further from resonance, owing to spontaneous scattering of the far red-detuned laser field, the heating should be considered as the dominant reason for atom loss from the atom trap. To quantify the effect, we should confirm the scattering rates. Hence, for Rb, the scattering rate, for an atom in a dipole trap is given as<sup>[15]</sup>

$$\Gamma_{\text{sc}}(\mathbf{r}) = \frac{1}{\hbar\epsilon_0 c} \text{Im}(\alpha) I(\mathbf{r}) = \frac{3\pi c^2}{2\hbar\omega_0^3} \left(\frac{\omega}{\omega_0}\right)^3 \times \left(\frac{\Gamma}{\omega_0 - \omega} + \frac{\Gamma}{\omega_0 + \omega}\right)^2 I(\mathbf{r}). \quad (5)$$

Here,  $c$  is the speed of light,  $\omega_0$  is the frequency at resonance,  $\hbar$  is the reduced Planck constant, and  $\Gamma$  is the damping rate. According to Eq. (5), the result shows that the maximum photon scattering rate of Rb atoms in the optical trap is lower than 1/s.

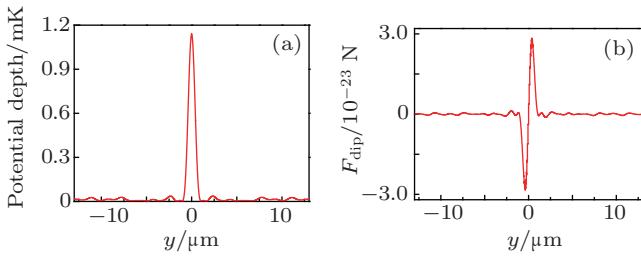


Fig. 5. (color online) (a) Potential depth along the  $y$  direction, and (b) the dipole force exerted on atoms in the laser field along the  $y$  direction.

### 3.2. Van der Waals attraction to the surface

For the structure with a size of a few micrometers, when the trapped atom is near the dielectric surface, atom-solid state interaction becomes important. The Van der Waals potential may shift the trap minima. To quantify this effect, we use the Lennard-Jones (LJ) potential as an approximation,<sup>[19]</sup>

$$V_{\text{vdw}} = -\frac{C_3}{d^3}, \quad (6)$$

$$C_3 = \frac{3(\epsilon_r - 1)}{16(\epsilon_r + 1)} \lambda^3 \hbar \Gamma. \quad (7)$$

Here  $\epsilon_r$  is the relative dielectric constant of the surface,  $\lambda = 1.55$   $\mu\text{m}$  and  $\Gamma/2 = 6$  MHz, respectively, are the incident wavelength and natural linewidth of the dominant transition from the ground state (for  $^{87}\text{Rb}$  atom). For metals or high-index dielectrics such as silicon, the factor  $(\epsilon_r - 1)/(\epsilon_r + 1)$  is approximately one. Taking the value 0.85 for silicon, we obtain  $= 2.5$   $\text{Jm}^3$ . According to Eqs. (6) and (7), we can calculate Van der Waals potential to the surface of the ring grating reflector. Figure 6 shows that Van der Waals potential has a low

effect on trapped atoms, which can be in favor of forming a stable dipole trap.

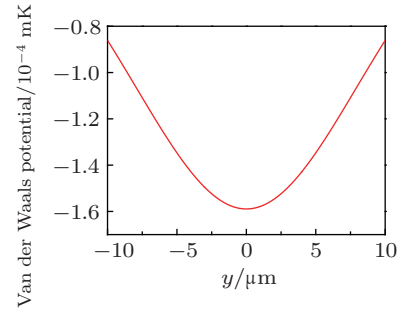


Fig. 6. (color online) Van der Waals potential for an atom located in the optical trap.

### 3.3. Microtrap array on a dielectric chip

The 2D concave grating reflector not only has high reflectivity and a wide wavelength-tuning bandwidth, but also obtains excellent focusing ability. Figure 7 shows the schematic representation of the microtrap array on the optical atom chip. The cold cloud of Rb atoms released from magneto-optical trap is prepared above the focusing region, which is located at 10.5  $\mu\text{m}$  away from the surface of the grating reflector. When cold atoms are loaded into a 2D array of laser traps, a novel 2D optical lattice with a tunable lattice constant, which is similar to 2D standing-wave optical lattices, can be formed. Its lattice constant can be tuned to be far larger than the one of a standing-wave optical lattice. Such a microtrap array can also capture the dielectric spheres, metal particles, and living cells.<sup>[20]</sup>



Fig. 7. (color online) Schematic diagram of the microtrap array of the curved grating reflector.

In addition, we also compare the focusing capability of our curved grating device with that of a perfect Si parabolic reflector, it is found that the perfect reflector can offer the same focusing performance, and its optical intensity at the focal point is enhanced by 40% compared with that of our curved grating reflector. For the fabrication of the perfect reflector with the parabolic smooth surface and micrometer size, it is harder than that of our curved grating structures proposed here. Our structures are processed by using electron-beam patterning followed by deep reactive-ion etching, which results in silicon pillars,<sup>[6,21]</sup> thereby showing that the curved grating reflector is an effective focusing device.

## 4. Conclusions

In this paper, we propose a novel scheme of strong optical confinement for cold atoms based on the concave grat-

ing structure. Our study shows that the grating reflector not only has high reflectivity and a wide wavelength-tuning bandwidth, but also exhibits high focusing ability. Under the incident polarized ( $1.55\ \mu\text{m}$ ) illumination, the grating reflector with a diameter of  $15.2\ \mu\text{m}$  can generate a focal spot with  $10.5\text{-}\mu\text{m}$  focal length and  $0.89\text{-}\mu\text{m}$  FWHM. In addition, such a focusing optical field reflected from the curved grating structure can provide the deep potential to trap the Rb cold atoms released from a standard magneto-optical trap with a temperature of  $120\ \mu\text{K}$ , and the maximum photon scattering rate in the optical trap is lower than  $1/s$ . Our scheme can be used to construct various surface optical micro-structures to trap cold atoms. Such a microtrap array can also manipulate and control cold molecules, or microscopic particles such as dielectric spheres, metal particles, and living cells.

## References

- [1] Tibuleac S and Magnusson R 1997 *J. Opt. Soc. Am. A* **14** 1617
- [2] Zhou Y, Huang M C Y and Chang-Hasnain C J 2008 *IEEE Photon. Technol. Lett.* **20** 434
- [3] Chase C, Rao Y, Hofmann W and Chang-Hasnain C J 2010 *Opt. Express* **18** 15461
- [4] Duan X, Huang Y, Ren X, Shang Y, Fan X and Hu F 2012 *IEEE Photon. Technol. Lett.* **24** 863
- [5] Lv Q, Pan P, Ye H, Yin D, Wang Y, Yang X and Han Q 2016 *Chin. Phys. B* **25** 38505
- [6] Nshii C C, Vangeleyn M, Cotter J P, Griffin P F, Hinds E A, Ironside C N, See P, Sinclair A G, Riis E and Arnold A S 2013 *Nat. Nanotechnol.* **8** 321
- [7] Huang M C Y, Zhou Y and Chang-Hasnain C J 2007 *Nat. Photon.* **1** 119
- [8] Fattal D, Li J, Peng Z, Fiorentino M and Beausoleil R G 2010 *Nat. Photon.* **4** 466
- [9] Lu F, Sedgwick F G, Karagodsky V, Chase C and Chang-Hasnain C J 2010 *Opt. Express* **18** 12606
- [10] Klemm A B, Stellinga D, Martins E R, Lewis L, Huyet G, O'Faolain L and Krauss T F 2013 *Opt. Lett.* **38** 3410
- [11] Lee J H, Yoon J W, Jung M J, Hong J K, Song S H and Magnusson R 2014 *Appl. Phys. Lett.* **104** 233505
- [12] Yu J, Ma H, Wang J, Li Y, Feng M and Qu S 2015 *Chin. Phys. B* **24** 098102
- [13] Duan X, Zhou G, Huang Y, Shang Y and Ren X 2015 *Opt. Express* **23** 2639
- [14] Yang B, Li Z, Yu Y and Yu J 2014 *Chin. Phys. B* **23** 114206
- [15] Grimm R, Weidemüller M and Ovchinnikov Y B 2000 *Adv. At. Mol. Opt. Phys.* **42** 95
- [16] Karagodsky V and Chang-Hasnain C J 2012 *Opt. Express* **20** 10888
- [17] Collin S 2014 *Rep. Prog. Phys.* **77** 126402
- [18] Chang-Hasnain C J and Yang W 2012 *Adv. Opt. Photon.* **4** 379
- [19] Landragin A, Courtois J Y, Labeyrie G, Vansteenkiste N, Westbrook C, and Aspect A 1996 *Phys. Rev. Lett.* **77** 1464
- [20] Kim J D and Lee Y G 2014 *Biomed. Opt. Express* **5** 2471
- [21] McGilligan J P, Griffin P F, Riis E and Arnold A S 2015 *Opt. Express* **23** 8948